LOW ENERGY HYDROGEN SENSOR

Linke, S.[1], Dallmer, M.[1] Werner R.[2] and Moritz, W.[1]
[1] Humboldt University of Berlin, Brook-Taylor-Str.2, Berlin, 12489, Germany,
sebastian.linke@hu-berlin.de
[2] OUT e.V., Köpenicker Str. 325, Haus 201, Berlin, 12555, Germany,

ABSTRACT

A new silicon based hydrogen sensor for measurements at high concentrations near the lower flammable limit of hydrogen (40,000 ppm) is presented. Due to operation at room temperature the power consumption of the sensor is by several orders of magnitude smaller than that of other sensors on the market. Further development of the sensor system could lead to battery powered or even energy-independent operation. As sensor fabrication is based on semiconductor technology, low cost production can be achieved for the mass market. The sensor investigated showed good long-term stability combined with a fast response on the basis of cyclic thermal activations. This was demonstrated by a stress test that simulated the activation and measurement cycles experienced by the sensor in one year. Finite element method was used to further reduce the power consumption of the thermal activation. This resulted in an average power consumption of 2×10^{-6} W for the sensor activation.

1. INTRODUCTION

Hydrogen production via electrolysis is one of the most promising ways for storing energy. Primary energy produced from renewable sources like sun power or wind is discontinuous and needs energy storage for higher efficiency. Beside the energy storage function there will be an increasing number of direct applications of H_2 like H_2 powered cars or fuel cells. Many of these applications will be in direct contact to the customer.

The high risk of explosion has lead to efforts for increasing the security in handling of H_2. An important aspect is the availability of sensors for the detection of H_2. The Lower Flammable Limit (LFL) for H_2 in air is very low i.e. concentrations of only 4%. A wide acceptance of H_2 technologies in general will only occur if H_2 is as safe as conventional fuels. Unfortunately, H_2 as the smallest molecule is challenging to detect in small quantities, and the human body is not able to sense H_2 at all. In Europe it is state of the art that a H_2 sensor should give a fast and reliable indication of danger at values of 20% of the LFL (8,000 ppm) and a final alarm at values of 40% LFL (16,000 ppm). Hence the concentration range from 4,000 ppm to 40,000 ppm is of interest for LFL detection.

In the literature many different H_2 sensing methods and sensors have been described. Boon-Brett et al [1] divided the available H_2 sensors in seven different types using their different transducers methods. In particular electrochemical [2], semiconducting metal-oxide [3], catalytic [4], thermal conductivity [5], metal-insulator semiconductor MIS [6], optical [7] and combined [8] sensor technologies are available. Based on the risks of H_2, a sensor for H_2 should fulfil many requirements. First of all the sensor should be able to detect H_2 concentration below the LFL. Secondly, the sensor performance must be adequate to give a fast sensor response if the H_2 concentration suddenly increases. Furthermore, the energy consumption is of special interest for battery-powered sensors used in the home. In the future when it comes to the development of energy autarkic H_2 sensors, energy budget is even more critical. Until now, most of the available H_2 sensors are working above room temperatures and/or require extra power for their transducers.

Recently we reported a H_2 sensor based on a $Pd/LaF_3/Si_3N_4/SiO_2/Si$-field effect structure using lanthanum fluoride as a solid electrolyte [9]. In contrast to the widely used field-effect H_2 sensors [10], our sensor is able to work at room temperature and is based on simple capacitive measurement. To guarantee long-term stability, a cyclic thermal activation was developed to preserve fast H_2 responses. In other experiments, we showed that heat impulses of less than 1 ms are sufficient to activate a

similar sensor structure [11]. This reduces the power consumption to less than 10^{-8} W for one activation per day. Using a single 9V battery this leads to a sensor life time of several years.

There are two different types of field-effect transducers [12]: transistors and capacitive Metal Insulator Semiconductor structures (MIS): transistors and capacitive Metal Insulator Semiconductor (MIS) structures. For a MIS structure, the high-frequency Capacitance-Voltage (CV) curve is shown in Fig. 1. If H_2 is present, the CV curve is shifted towards negative voltages. The reason for that shift can be explained as follows.
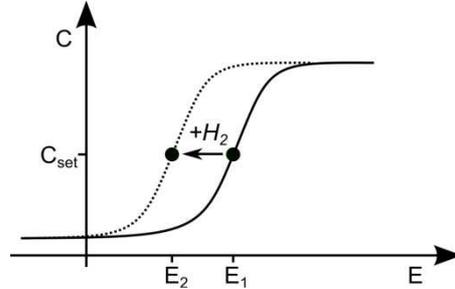

Figure 1. Capacitance Voltage curve of an Metal Insulator Semiconductor structure in air (solid line) and after adding of H_2 (dotted line)

Palladium is often used in H_2 sensors because of its ability to absorb H_2 at room temperature [13]. As a result Pd is used as the gate material in H_2 sensing field-effect sensor. H_2 absorbs at the Pd surface and is split into atomic hydrogen. The hydrogen atoms can than enter the Pd lattice. Within, the lattice hydrogen moves with a diffusion coefficient of 4×10^{-7} cm^2/s at room temperature (α phase) [13]. For MIS structures using no solid electrolyte, the atomic hydrogen induces a dipole layer at the Pd/Insulator interface [14]. Using a structure with a solid electrolyte e.g. lanthanum fluoride, the main reaction takes place at the three phase boundary Pd/solid electrolyte/air. We suggested a mechanism based on the Oxygen sensing ability of the lanthanum fluoride layer [9]. Oxygen adsorbs at adsorption sites A* at the triple interface (1) and reacts with water forming OH$^-$ (2). The high mobility of OH$^-$ in the LaF$_3$ lattice (3) stabilises the OH$^-$ formation. H_2 can now reduce the surface Oxygen O_2(A*) concentration by producing water (4).

$$O_2 + A^* \rightleftarrows O_2(A^*) \tag{1}$$

$$O_2(A^*) + H_2O + e^- \rightleftarrows HO_2(A^*) + OH^- \tag{2}$$

$$OH^- + (F^*) \rightleftarrows OH^-(F^*) \tag{3}$$

$$O_2(A^*) + 2H_2 \rightleftarrows 2H_2O(A^*) \tag{4}$$

The oxygen dependence is no drawback since the O_2 concentration is sufficiently constant under ambient conditions. Another difference of MIS sensors with and without solid electrolyte is the different concentration sensitivity. The solubility of H_2 in metals follows Sievert's law with a square root dependence [15]. Therefore the signal is proportional to the square root of the hydrogen concentration and reaches saturation at about 2,000 ppm [16]. In contrast, using LaF$_3$, the reaction takes place at the three phase boundary. This reaction is more complex and leads to Nernstian behaviour. Therefore our sensor has a logarithmic concentration dependence. What both MIS structures have in common is the fact that the surface reactions add additional positive charges to the interface leading to a concentration dependent gate voltage. As a result, the CV curve is shifted to lower voltages (Fig.1).

Different methods can be used for the monitoring the shift of the CV curve. Commonly the voltage is set to a constant value in the steep region of the CV curve. If the CV curve is shifted towards negative voltages an increase in the capacitance is measured (for n silicon). Hence the shift of the CV curve along the voltage axis can be calculated from the change in capacitance. This method is suitable for small voltage changes that do not cause the applied voltage to move outside the steep region of the CV curve. Another way is to keep the capacity constant by adjusting the voltage via a feedback controller.

This method is slower because a feedback from the sensor is needed but no recalculation is necessary and it is even accurate for large voltage shifts.

In this paper, the application of the Pd/LaF$_3$/Si$_3$N$_4$/SiO$_2$/Si-field-effect sensor to the alarm level detection of hydrogen will be shown. The improvement of long term stability based on short thermal impulses is demonstrated and proven by a stress test. Furthermore, thermal simulations of the heat distribution in the silicon are discussed.

2. EXPERIMENTAL

The sensor consists of a thin layer structure based on the semiconductor/insulator substrate shown in Fig.2. The substrate is a phosphorus doped silicone with a carrier concentration of 10^{16} cm^{-3}. The insulator, which is composed of SiO$_2$ and Si$_3$N$_4$ (both 50 nm thick) was produced using standard semiconductor techniques. A layer of 150 nm LaF$_3$ was deposited by thermal evaporation under high vacuum. The 20 nm thick Pd film was produced by DC sputtering in argon at 1 Pa and a deposition rate of 1 nm s^{-1}. The Pd sensor area was structured via a shadow mask. For electrical contact, aluminium was deposited by electron beam physical vapour deposition on the back of the silicon substrate.
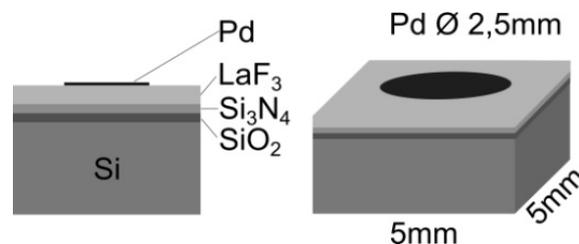

Figure. 2. Sensor layout. Si substrate with SiO$_2$ (50 nm), Si$_3$N$_4$ (50 nm), LaF$_3$ (150 nm) and Pd (20 nm) layers.

The measurement setup is illustrated in Fig. 3. Mass flow controllers were used to adjust the concentration by mixing synthetic air with different concentrations of hydrogen (up to a maximum of 30,000 ppm in synthetic air). The flow rate was kept constant at 100 ml min^{-1}. It should be pointed out that the H$_2$ concentration in synthetic air is usually in the range of 0.1 ppm; hence concentrations below 0.1 ppm are not detectable.
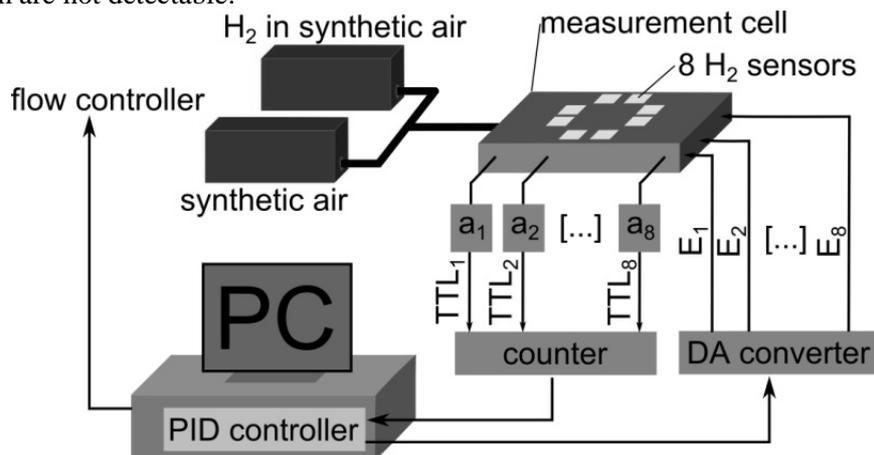

Figure 3. Measurement setup for the detection of H$_2$. Up to 8 sensors were measured in parallel using 8 ICM7555 timer based circuits (a$_1$-a$_8$) and a multiple counter. The TTL signal representing the capacitance is kept constant for every sensor by adjusting the potential. This was achieved using a software based feedback controller (PID controller).

For the measurement of the capacitance different methods were used. Single sensors were measured with Hewlett Packard 4284A type LCR meter. The frequency of the 10 mV superimposed AC signal was set to 10 kHz. The capacitance was kept constant by means of a software feedback controller provided by the National Instruments software LabView. In addition, up to 8 sensors could be

measured parallel via a circuit, based on an ICM7555 timer. The TTL response of the timer reflects the possibility to charge and discharge the sensor capacity at a rate of 100,000 kHz. A triggered counter (MCC USB-4303) was used to read the TTL frequency and a D/A converter (MCC USB 3103) for applying the gate voltages for each sensor. Again a LabView based feedback program was set up to keep the capacitance constant. A relative humidity of 100% was established by bubbling the test gases through purified water. Afterwards, the saturated and dry test gases were mixed to obtain different relative humidities.

3.0 RESULTS

3.1 Sensor Response

The sensor response to different concentrations of H_2 is shown in Fig. 4a. The relative humidity was set to 50% (the relative humidity in a typical working environment is known to be between 40-65%). Furthermore the sensor signal follows, as stated earlier [9], a logarithmic behaviour. The sensitivity is typically about 150 mV/decade H_2 (Fig. 4b). With a t_{90} time of 4 s for 8,000 ppm (Fig. 4c) the sensor reacts reasonably fast, even though the measurement was not optimised for rapid kinetic response.
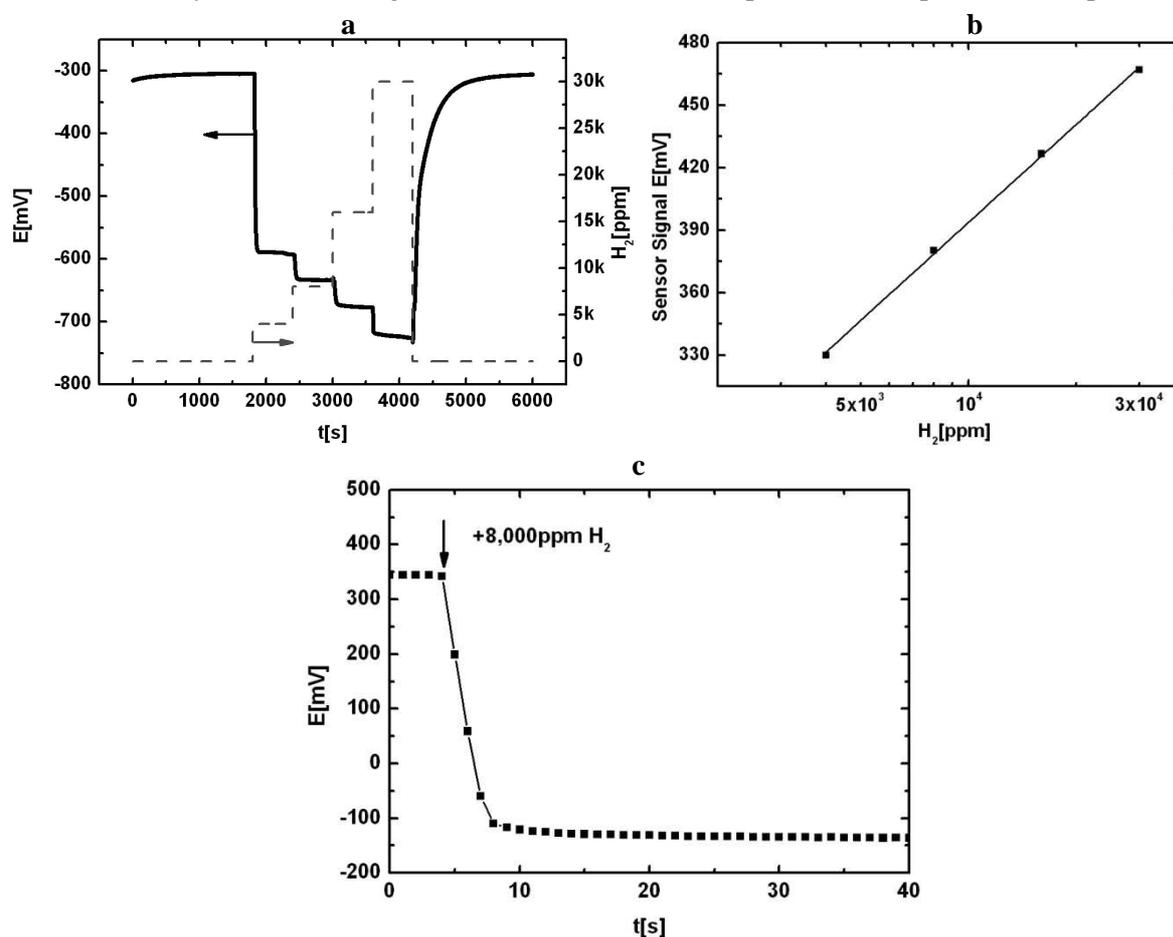

Figure 4, Sensor response (solid line) for different H_2 concentrations in air (dashed line) and constant relative humidity of 50% after activation. 4b) The sensor signal versus H_2 concentration taken from 4a. 4c) The kinetic response of the sensor to 8,000 ppm H_2 in air from a baseline of air in 50% humidity. A measurement point was recorded every second.

Apart from the higher H_2 concentration needed for LFL detection, the LaF_3 based field effect sensor is capable of measuring concentrations from a few ppm up to several percent of H_2 [9]. The sensor signal for 100 ppm immediately after preparation of the sensitive layers is shown in Fig. 5. After 10 days, the signal level remained constant while the dynamic behaviour is much slower (Fig. 5). To overcome that problem a short heat treatment was shown to be effective. For that purpose, the sensor is heated to a temperature between 400 K and 550 K for less than 100 s. Since the auto ignition temperature of H_2 is

above 770 K there is no risk of auto ignition. As a result of the thermal treatment the sensor response is as fast as for the freshly prepared sensor.
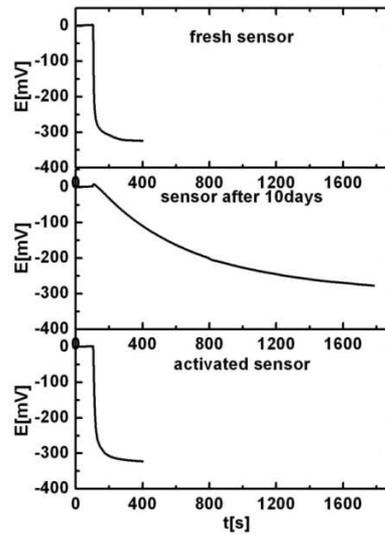

Figure 5, Comparison of the sensor response at 100 ppm H_2 in air for a freshly prepared sensor with the sensor after 10 days stored in air and the reactivated sensor.

In Fig. 6 the long term behaviour of the sensor was investigated using a stress test. A cycle of thermal activations and H_2 measurements at the first alarm level (8,000 ppm) simulated the conditions experienced by a sensor in about one year (330 days) by reducing the cycle time from 24 to one hour. In Fig.6a, the reproducibility of the hydrogen signal is shown for cycles 2, 50, 150 and 300 respectively. In Fig. 6b, the signal for 330 measurements is given. A stable signal difference between air (50 min desorption) and 8,000 ppm hydrogen of 424 mV with a standard deviation of 8 mV was found (Fig. 6b).
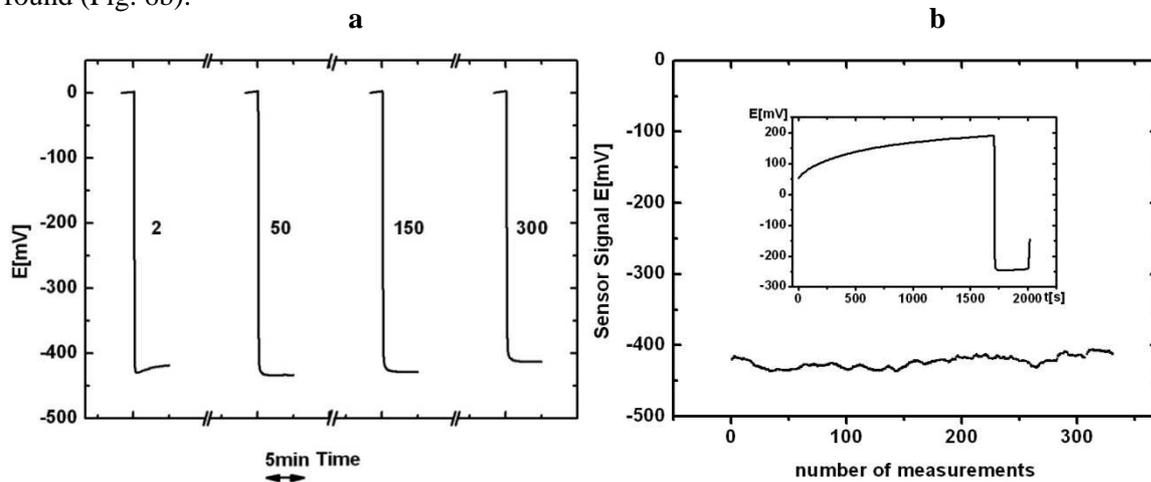

Figure 6, Stress test simulating the behaviour of a H_2 Sensor for 330 days. For the measurement the sensor was activated 330 times, cooled down and measured at 8,000 ppm. 6a) The sensor response after different activating steps. 6b) The sensor signal for all measurements. The insert shows the points (dots) that were used to calculate the signal for a single measurement.

3.2 Thermal simulation

Further investigation focused on the optimization of the activating procedure. The aim was to reduce the energy consumption for the thermal treatment. Therefore, Finite Element Method (FEM) was used to analyse the heat dispersion after the power pulses. The investigation included the standard sensor layout, different heating structures, time dependencies and the natural convective air flow. A model of a Si/SiO_2 based multi layer sensor with a Pd gate and LaF_3 as solid electrolyte was set up. The

structure geometry favoured by simulations was a 3x3 mm, 390 μm thick Si chip with thinned Si membranes of 30 μm thickness. This volume reduction to 16.5 % of the formerly used 5x5 Si volume was the first step to save energy. The Pt thin film heater was placed in a circuit around the sensitive Pd gate Fig.7.
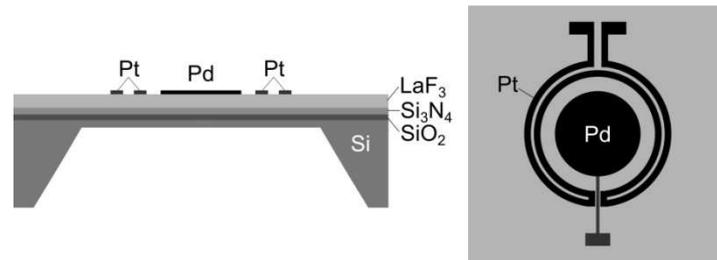

Figure 7 Sensor structure for FEM analyses.

Several geometries of heaters were investigated to find the one with the optimum properties. When heating duration was lowered from 1 s down to 1 ms the energy demand was lowered from 0.38 J to 0.08 J, while the required peak power rises from 3.8 W to 86 W. The disadvantage of heat pulses shorter than 10 ms is the undefined temperature allocation within the sensitive Pd-gate layer and the high power input demand for a short time.
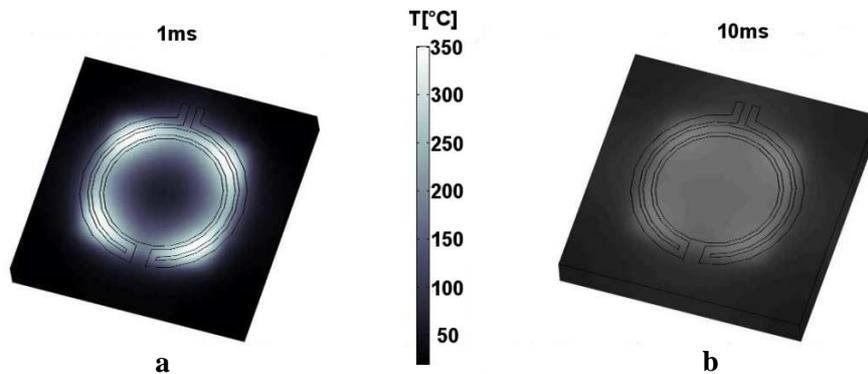

Figure 8. Simulating heat pulse to a H_2 sensor (3x3 mm Si: 390 μm /30 μm membrane) for 1 ms pulse at time 1 ms (a) and 10 ms pulse at time 10 ms (b)

The high power input at 1 ms leads to a high temperature gradient in the sensitive layer (Fig 8a). The effect of an inhomogeneous activation temperature is detrimental to the sensor performance. Therefore, it is desirable to have a reduced temperature gradient of no more than 20 degrees throughout the Pd-region to grant reliable functionality of the H_2 alarm sensor. As seen in Fig. 8b, a compromise between the heating time (10 ms) and energy demand (0.2 J) was found with a small temperature gradient in the sensitive area. When using shorter heating times, only the membrane is heated. As a result an average power consumption of only 2×10^{-6} W (one activation per day) is established. This enables our H_2 sensor to be used in battery powered systems. Hence a typical 9 V battery with 250 mAh can provide energy for theoretically at least 100 years of activations.

In further experiments the theoretical approach was investigated in a real sensor device. An electrolyte capacitor was used for the necessary power output to the Pt heater. The actual temperature of the heater was calculated from the change of the Pt-resistance. A 10 ms heating pulse with a power input of around 50 W granted an adequate temperature and heat circulation for the reactivation of the sensor.
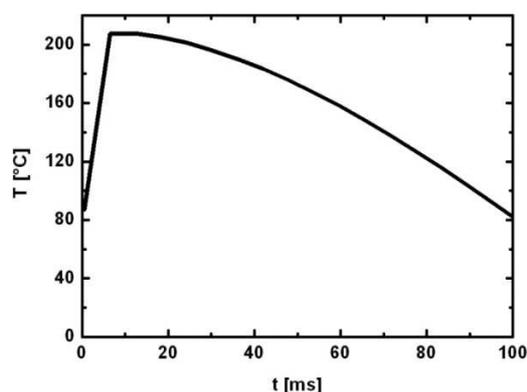
Figure 9. Measured heat-up and heat dissipation process of a sensor (3x3 mm) at a 10 ms heat pulse from a circular Pt thin film heater (around 50 Ohm)

4.0 CONCLUSION

We could show that a H_2 sensor based on a Pd/LaF$_3$/Si$_3$N$_4$/SiO$_2$/Si-field-effect structure is able to detect H_2 in the concentration range essential for the Lower Flammable Level warning. Furthermore our sensor is able to provide long time stable signals with fast kinetics for at least one year via cyclic activations. Using FEM simulations, the sensor structure and the process of thermal activation could be optimised in order to lower the power consumption of the sensor. As a result, our H_2 sensor (in contrast to most other H_2 sensors) is able to work with a battery based energy supply.

REFERENCES

1   Boon-Brett, L. Bousek, J. Black, G. Moretto, P. Castello, P. Hübert, T. Banach, U., Identifying performance gaps in hydrogen safety sensor technology for automotive and stationary applications. *International Journal of Hydrogen energy,* **35**, 2010, pp. 373-384

2   Korotcenkov, G. Do Han, S. Stetter, J. R., Review of electrochemical hydrogen sensors. *Chemical Reviews*, **109**, 2009, pp. 1402-1433

3   Aroutiounian V., Metal oxide hydrogen, oxygen and carbon monoxide sensors for hydrogen setups and cells. *International Journal of Hydrogen Energy*, **32**, No. 9, 2007, pp. 1145-1158

4   Han, C. H. Hong, D. W. Han, S. D. Gwak, J. Singh, K. C., Catalytic combustion type hydrogen gas sensor using TiO2 and UV-LED. *Sensors and Actuators B*, **125**, 2007; pp. 224-228

5   Simon, I. Arndt, M., Thermal and gas-sensing properties of a micromachined thermal conductivity sensor for the detection of hydrogen in automotive applications. *Sensors and Actuators A*, **97-98**, 2002, pp. 104-108

6   Lundström ,I., Hydrogen sensitive MOS-structures: part 1: principles and applications. *Sensors and Actuators*, **1**, 1981, pp. 403-426

7   Sumida, S. Okazaki, S. Asakura, S. Nakagawa, H. Murayama, H. Hasegawa, T., Distributed hydrogen determination with fiber-optic sensor. *Sensors and Actuators B: Chemical*, 2005; **108**, pp. 508-514.

8   Thomas, R. C., Hughes, R. C., Sensors for detecting molecular hydrogen based on Pd metal alloys. *Journal of The Electrochemical Society*, **144**, No. 4, 1997, pp. 3245-3248

9   Moritz, W., Fillipov, V., Vasiliev, A., Cherkashinin, G., Szeponik, J., A Field Effect Based Hydrogen Sensor for Low and High Concentrations, *ECS Transactions*, **3**, 2006, pp. 223-230

10   Lundström, I., Armgarth, M., Petersson, L.-G., Physics with catalytic metal gate chemical sensors, *Crit. Rev. Solid State Mater. Sci,*. **15,** 1989, pp 201–278

11   Moritz, W., Roth, U., Heyde, M., Rademann, K., Reichling, M., Hartmann, J., Submicrosecond range surface heating and temperature measurement for efficient sensor reactivation, *Thin Solid Films*, **391**, 2001, pp. 143-148

12   Sze, S. M., Kwok, K. N., Physics of Semiconductor Devices. 2006, John Wiley & Sons, New York

13   Alefeld, G., Volkl, J., Diffusion of hydrogen in metals, Hydrogen in Metals, Vol. 1, Springer Verlag, New York,, 1978, pp. 321-348

14   Lundström I, Shivaraman M S, Svensson C M. A hydrogen sensitive Pd-gate MOS transistor, *Journal of Applied Physics*, **46**, 1975, pp. 3876-3881

15   Wicke E, Brodowsky H, Züchner H. Hydrogen in Palladium and Palladium Alloys, Hydrogen in Metals, Vol 2, Springer Verlag, New York, 1978, pp. 73-155

16   Eriksson M., Salomonsson A., Lundström I., Briand D., Abom A. E. The influence of the insulator surface properties on the hydrogen response of field effect sensors. *Journal of applied Physics*, **98**, No. 3, 2005, pp 034903-6